

A novel voltage sag approach during unintentional islanding events: A survey from real recorded events

Alexandre Serrano-Fontova^{1,2}, P. Casals-Torrens¹ and R. Bosch¹

¹ Department of Electrical Engineering
E.T.S.E.I.B, Polytechnic University of Catalonia
Edifici H planta 2, Avda. Diagonal, 647 08028 Barcelona (Spain)

² Electrica Serosense Distribuidora
Pol. Ind. Panamá. Ctra. Nac. II Km. 450, 25110 Torres de Segre (Spain)

Abstract. In this paper, a new voltage sag approach is proposed, analytically modelled and validated by both simulation and field measurements. The main aim of this approach is to propose a new voltage sag approach, which appears during unintentional islanding operations (IOs) [1]. The unintentional IO occurs when an induction motor is removed from the main utility following a circuit breaker (CB) fault clearing, transiently, the induction motors (IM) are acting as generators maintaining the affected distribution feeder with voltage until it is reconnected. The modelled voltage sag in the current article follows an exponential form, in fact, here it will be demonstrated that the proposed model reaches satisfactorily the field measurements and evidences the dependability of the model adopted. Furthermore, it is worthwhile to note that this novel power quality (PQ) event has not been investigated yet and enhances the current voltage sag studies. Lastly, it is crucial to point out that all recorded events and the large amount of data needed so as to validate this transient, has been measured in a distribution network (DN) located in Spain.

Key words

Power quality, islanding operations, voltage sags, distribution networks.

1. Introduction

The PQ has become a topic of undeniable scientific scrutiny due to the increasing use of sensitive equipment as well as the need of power supply continuity in both companies and end-users. Hence, many attempts have been conducted in order to define and characterise the main features of the PQ. Particularly, referring to voltage sags, are defined as a decrease in the voltage between 0.1 to 0.9 p.u. in rms voltage at the rated frequency during between 0.1 s to 1 s [2]-[4]. Crucially, voltage sags are of utmost importance in the PQ studies and many efforts have been made so as to locate its origin [5], predicting its effects into loads and generators, as in [6]-[10]. Notwithstanding the foregoing, the load immunity is still under scientific study considering that same voltage sag deep and duration has different effects towards sensitive loads [11],[12]. Voltage sags can be caused by numerous events such as, short-circuits, IM reacceleration [13], IM starting [14], or sudden loads connection. Against this background, voltage sags,

generally, can be classified by its duration and deep [15]. In the early studies, voltage sags were considered rectangular, afterwards it was found that a distinction between discrete and abrupt could be made in regards of its beginning and recovery considering the phase angle jump [16]. On the other hand, an interesting insight towards PQ studies is done when part of the grid is isolated from the main utility, conceptually known as IOs, therefore, the PQ in smart grids and isolated areas has reignited an undeniable fruitful debate [17]-[19]. Particularly, in these scenarios, sensitive loads may undergo undesirable large and hazardous disturbances. Therefore, the detection and clearance of this unexpected IOs as stated in [20], is vital. Usually, IOs occur in presence of distributed generation (DG) resources, nonetheless, in the present approach, the aforementioned IO is caused by the IMs inertia following the loss-of-mains takes place, where is reasonable to expect an interruption [13].

In the present paper, a new exponential voltage sag is proposed, its depth and duration depend on the rate between the induction motors rated power, on the feeder loads, on the type and value of the load torque applied to the induction motors, crucially depend on the preset reclosing time considered at the CB substation as well as on the type of fault. Moreover, this proposal enhances the current available voltage sags modelling and further investigates the behaviour of this unexpected transient.

2. Voltage sags review

The general classification of voltage sags is thoroughly defined in [2]. Depending on the number phases involved in the disturbance, the duration and its deep, the following classification is detailed in the subsequent sub-section A. Thus, a comprehensive description of the voltage sags and its calculation is done in [21]. Since the nature of the faults is diverse, its recovery depends on the origin of the fault, and we can distinguish abrupt and discrete voltage sags. As commented earlier, voltage sags are characterized by its *type*, its *duration*, by its *deep* and finally by the *phase angle jump*. It is important to bear in mind that this parameters depend on the protective settings and also on

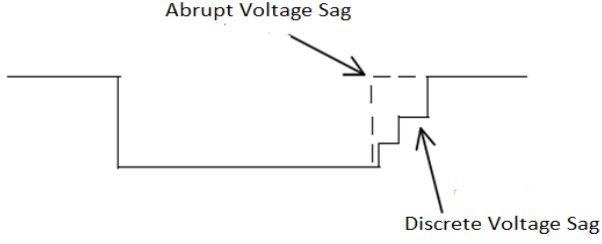


Fig. 1. Voltage sags current classification

the nature of the grid. Firstly, abrupt voltage sags are ones who recover directly and discrete voltage sags are those which recover with a time delay, as it can be seen in Fig. 1.

A. Current voltage sag classification

According to [22], the following classification can be done:

- Asymmetrical voltage sags due to single-line-to-ground (SLG) short circuits (Type B), or due to phase-to-phase (L-L) short-circuits (Types C and D).
- Three-phase currents involved at the fault, symmetrical voltage sags (Type A) and double-line-to-ground (L-L-G) short-circuits (E, F and G). This type recovers discrete with two steps, originating (A₁, A₂, E₁, E₂, F₁, F₂, G₁ and G₂).
- Three-phase short-circuits which involve three-phase and ground, originating a three-step recovering (A₁, A₂ and A₃).

3. Proposed voltage sag approach

This section is aimed at describing the novel voltage sag modelling, purposefully, it will describe the analytical expression. Since this type of disturbance is originated by the IMs, it is essential to recall its equations in order to fully define this electrical transient. The induction machine acting as a motor can be defined by this set of differential equations in the abc-reference frame (1):

$$\begin{bmatrix} v_{S abc} \\ v_{R abc} \end{bmatrix} = \begin{bmatrix} R_s & 0 \\ 0 & R_r \end{bmatrix} \begin{bmatrix} i_{S abc} \\ i_{R abc} \end{bmatrix} + \frac{d}{dt} \begin{bmatrix} \phi_{S abc} \\ \phi_{R abc} \end{bmatrix} \quad (1)$$

This equation in synchronous (three-phase) reference can be expressed as dq reference by means of Park transformation (2):

$$\begin{aligned} v_{sd} &= (R_s + L_s \frac{d}{dt})i_{sd} + M \frac{d i_{rd}}{dt} - L_s \omega \psi i_{sq} - M \omega \psi i_{rq} \\ v_{rd} &= (R_r + L_r \frac{d}{dt})i_{rd} + M \frac{d i_{sd}}{dt} - L_r (\omega \psi - \omega_m) i_{rq} - M \omega \psi i_{sq} \\ v_{sq} &= (R_s + L_s \frac{d}{dt})i_{sq} + M \frac{d i_{rq}}{dt} - L_s \omega \psi i_{sd} - M \omega \psi i_{rd} \\ v_{rq} &= (R_r + L_r \frac{d}{dt})i_{rq} + M \frac{d i_{rd}}{dt} - L_r (\omega \psi - \omega_m) i_{sd} - M \omega \psi i_{sq} \\ \Gamma_m - \Gamma_{res} &= J \frac{d \omega_m}{dt} \\ \omega_m &= \frac{d \theta_m}{dt} \end{aligned} \quad (2)$$

where the subtitles r and s are referred to rotor and stator, $d\phi/dt$ is the flux linkage derivative, v_{abc} is the voltage vector and i_{abc} current vector, M is the inductance matrix. The inductance matrix depends on the rotor position $M(\theta)$. Note, however, that in a single-squirrel cage induction machine, both v_{rd} and v_{rd} are set to 0.

It being understood that following CB disconnection from the main grid, the transient electromagnetic torque $T_{em,IM}$ developed by the machine acting as a generator depends on the dynamic torque, load torque and friction torque, we have the following expression (4):

$$\begin{aligned} T_{em,IM} &= f(T_r, T_b, J_t, \omega_{im}) \\ T_{em,IM} &= \frac{d\omega}{dt} J_t - (T_r + T_b) \end{aligned} \quad (4)$$

The decreasing IM speed is given hereunder (5):

$$\frac{d\omega}{dt} = - \frac{(T_r + T_b)}{J_t} \quad (5)$$

Accordingly, the mechanical power developed by the machine in the transient process is then computed as (6):

$$P_{m im} = T_{em} \times \omega_{im} \quad (6)$$

Thence, feeder loads act decelerating the IMs, thereby, its speed can be computed as (7):

$$\frac{d\omega_{im}}{dt} = \frac{\omega_o}{2H_{im}} [P_{m im} - P_{e load}(\delta_{im})] \quad (7)$$

where the subscript im denotes that all values listed before are now referred to IM, $P_{e load}$ is referred to the power loads at the target feeder H_{im} is the IM inertia, J_t is the sum of the IM inertia and the load inertia, T is the electromagnetic torque developed by the machine acting as a motor, T_r is the load torque, T_b is the friction torque which will be considered as 0.056 Nm-s and $T_{em,IM}$ is the torque developed by the machine as acting as a generator.

A. Voltage sag features

Since the voltage sag parameters are v_{sd} and v_{sd} the stator voltages, by solving eqns (2) considering no external excitation (CB has opened, the stator voltages will decay exponentially being represented by the form (8):

$$v(\frac{d\omega}{dt}) = v_o e^{\frac{d\omega}{dt}} \quad (8)$$

Thus, speed derivative is related with torque and feeder loads as computed in (7), v is the decreasing rms voltage profile during the disturbance expressed in p.u., v_o is the pre-fault voltage. Note, however, that under steady state, acting as a motor, its derivative is zero and, during the IO its value is negative. The subsequent points characterise this voltage sag;

- Its depth is represented by its residual voltage and is given by (8). The minimum depth is when the derivative is zero, so the voltage value is 1 p.u.
- Its duration is defined by the rapid reclosing, typically between 0.5 s and 1s. See, for instance, [23].

- Its discrete recovery, which takes place when the CB recloses.

4. Test system under investigation

A. Test system

The one-line diagram of the test system used to perform this study is depicted in Fig. 1, it is a radial DN fed from an HV/MV substation. The short-circuit capacity measured at the HV terminal is 1000 MVA. Note that the system tested in this paper consists of three-medium voltage (MV) feeders, and two sub-feeders, named A and B which belong to feeder 1 and are connected to the substation through L12. Crucially, the section object of study is within the sub-feeder A, formed by 8 MV nodes and 5 low voltage (LV) nodes, where the unintentional IO occurs. System parameters data are detailed in [1]. Furthermore, the measurements were recorded by the protective relays

located at both Pcc₁ and Pcc₂ in the sub-feeder A (both depicted in red in Fig. 1) with a sampling frequency of 512 samples per cycle with a pre-trigger of 100 ms and post-trigger of 300 ms. For more information about the oscillography functions of the protective relays, see [24].

B. Three-phase Matlab/Simulink model adopted

The test system model has been implemented in the MATLAB/Simulink environment [25], taking advantage of the toolbox SimPowerSystem. The three-phase model implemented is showed in Fig. 2 and has been performed in a computer with a processor of 3.6 GHz 8-core Intel i7 and 8 GB of RAM. The simulation has been conducted in a discrete mode with a fixed sample time of 50·e-6 s, the solver function used is ode8 based on Dormand-Prince eight-order (RK8) formula and the simulation time for all scenarios consists of 2 s. All the simulations have been performed with a single line-to-ground (SLG) fault with a fault resistance of 5 Ω at node 7.

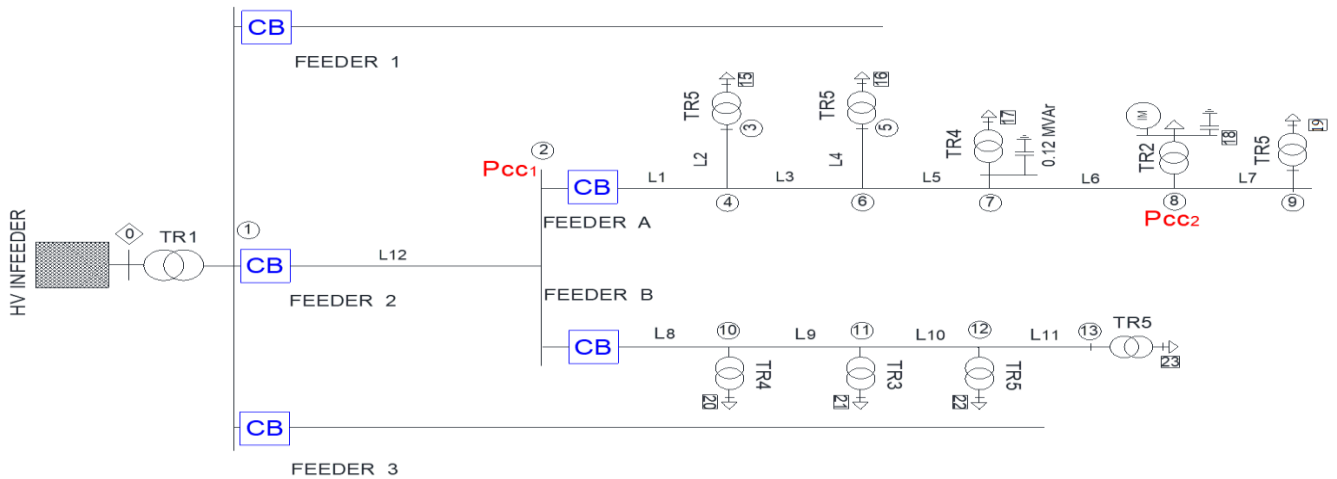


Fig.1. Test system under investigation

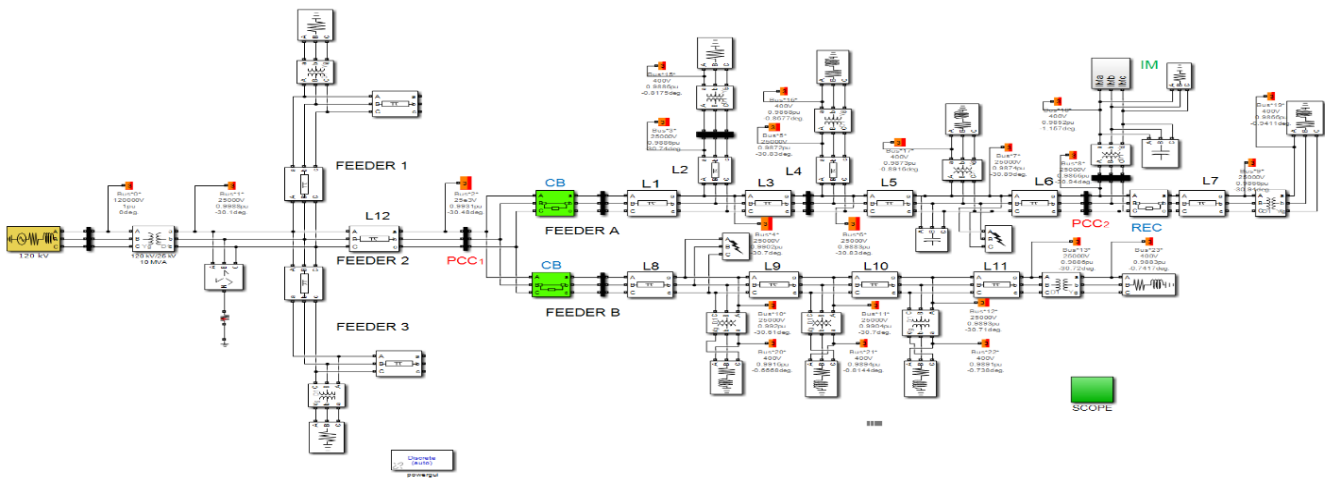


Fig.2. Three-Phase Matlab model adopted

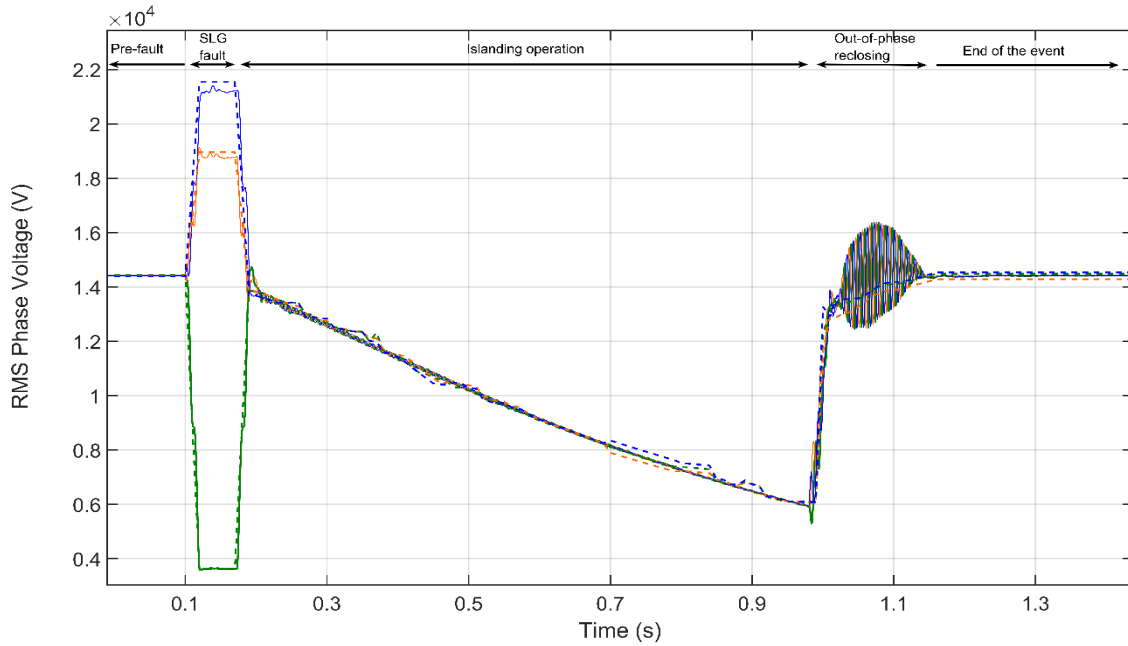


Fig.3 Model validation. RMS Phase voltage comparison, solid (simulation) / dashed (measurements), orange (Phase A), blue (Phase B) and green (Phase C)

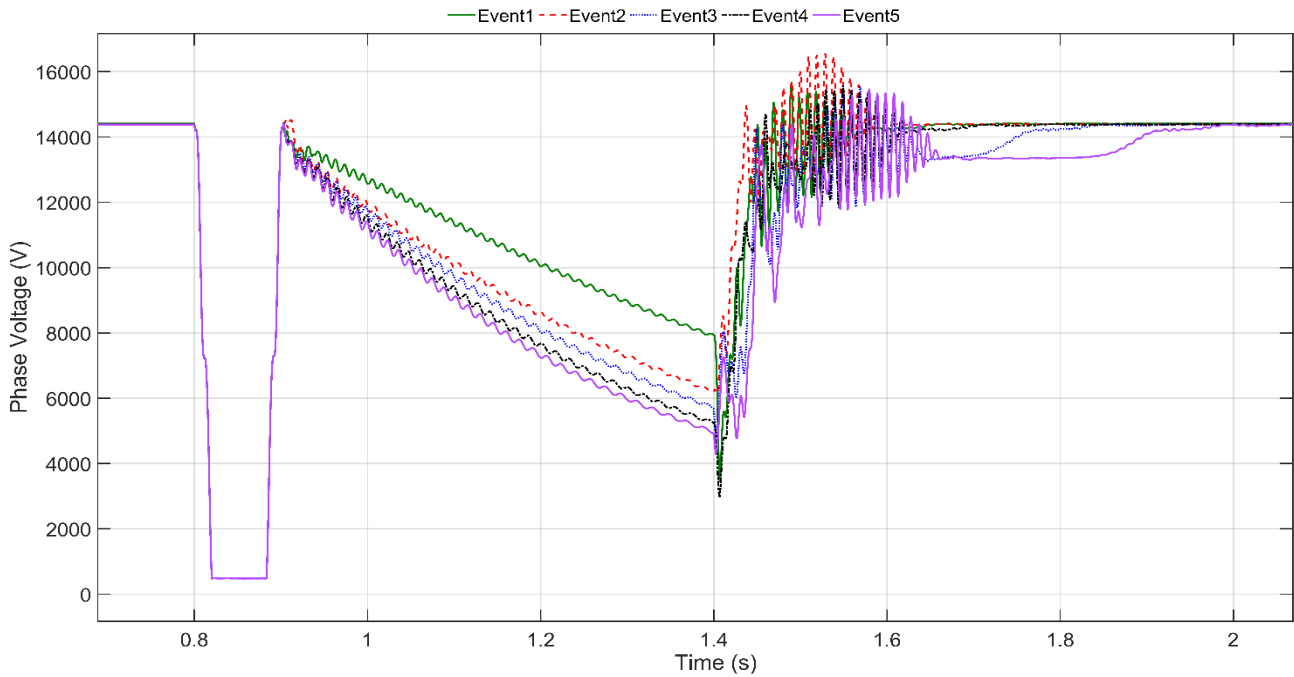


Fig. 4 Voltage sags profundity

5. Model validation and results discussion

This section is aimed at showing and discussing the previously proposed voltage sag approach as well as validating the model adopted by comparing both simulation results with field measurements.

A. Model validation

This sub-section seeks to address the validation of the three-phase Matlab/Simlink model adopted in order to give maximum fidelity not only to the recorded field measurements but also to the proposed model. For brevity purposes, the model validation will be made via one particular recorded event, in it, the comparison is made using the three-phase voltages, before, during and after IO takes place, see Fig. 3.

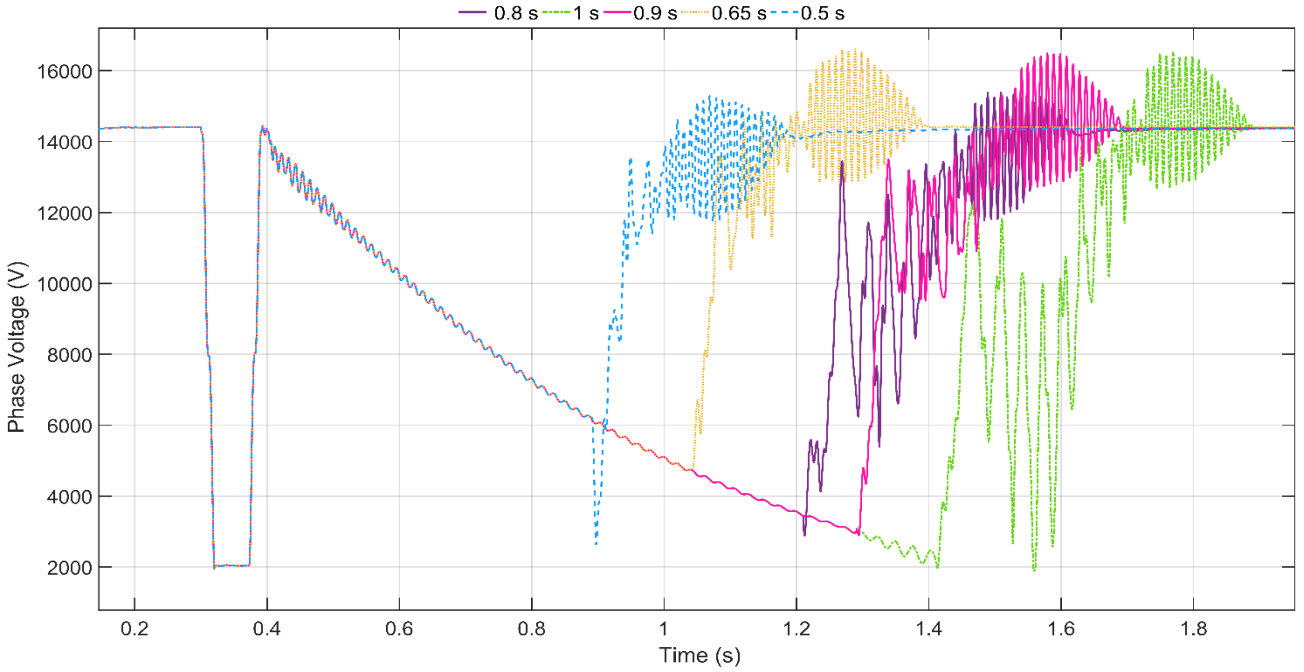


Fig. 5 Voltage sags duration

B. Simulation results and discussion

In the current sub-section, several simulations will demonstrate the previously described approach. Thus, in Fig. 4, several voltage sags are depicted obtained from the Matlab/Simulink performed simulations. Purposefully, voltage sags are represented, so as to observe its various profundities. As can be drawn from its simulations, the higher is loads active-power, the higher is its decreasing rate and consequently its profundity. On the other hand, Fig.5 unmistakably evidences the fact that voltage sags duration depends on the reclosing times implemented in the protective equipment. Thus, the simulation tested events will be discussed down below;

1) Voltage sag depth

From Fig. 4 it is observable that depending on the relation between the active-power loads and the IM active-power, the voltage sag can vary. Against this background, the higher is the imbalance, the higher is the voltage sag profundity, coinciding with low feeder loading levels and large IMs. Considering that the relationship between both powers is expressed with the non-dimensional coefficient γ and computed as in (9);

$$\gamma = \frac{P_{e,IM}}{P_{e,l}} \quad (9)$$

where $P_{e,IM}$ is the rated active-power of the IM and $P_{e,l}$ is the faulty feeder loads active-power both expressed in kW. Thus, event 1 represents a γ of 8, event 2 a γ of 4.2, event 3 a γ of 2.6, event 4 a γ of 1.6 and event 5 a γ of 1.45. In this sense, it is worth mentioning that the severest disturbances will occur when the coefficient is close to zero. Note, however, that for γ values higher than 8, the voltage value will follow the decreasing exponential curve, but the slop will be lower. Consequently, the voltage during the island will remain within acceptable limits. Furthermore, from the mechanical equation in the set of IMs equations (2), it can

be seen that the load torque can also influence the slope of the curves depicted in Fig. 4. A remarkable insight is the voltage recovery; it appears at $t = 1.4$ s when the CB preset reclosing of the feeder A takes place. Depending on the γ factor, the recovery takes longer. This fact is due to the high current absorbed product of the out-of-phase reclosing. The higher is the voltage mismatch between the grid and the island, the higher is the absorbed current, and the higher is the voltage recovery time.

2) Voltage sag duration

The voltage sag duration is observable in the four test simulations illustrated in Fig. 5. Thereby, the relationship between voltage sag duration and the protective settings has been demonstrated. From observing Fig. 5, it is seen that the same voltage recovery as in Fig. 4 appears, which, in turn, supports the three-phase adopted model. Nonetheless, it is essential to highlight the fact that, in the present paper only an SLG has been considered, but the type of fault and fault duration may affect the voltage during the island. This fact is due to the CB protective settings.

6. Conclusions

This paper has presented a new voltage sag typology; both simulations and real recorded events demonstrate the feasibility of the proposed analytical voltage sag approach. Purposefully, the results have proven the dependability of the adopted model, as well as the appropriateness of this new voltage sag approach. Overall, this study has enhanced the present research towards PQ disturbances. Furthermore, this study evidences the fact that further immunity tests are required in order to observe its effects into loads. Future research will be focused on validating the model feasibility with hardware-in-the-loop (HIL) simulations.

Acknowledgement

The authors wish to acknowledge the financial support and the willingness of sharing field measurements by the Spanish DSO Electrica Serosense Distribuidora. The authors would also like to thank the Catalanian College of Engineers for the grant received.

References

- [1] R. Bosch, P. Casals, and A. Serrano, "The influence of the self-excited induction machine into the electrical grid under instability situation - Real case measurement," *RE&PQJ*, vol. 1, no. 15, pp. 233–238, 2017.
- [2] M. H. Bollen, *Understanding Power Quality Problems*. 1999.
- [3] J. A. Martinez and J. Martin-Arnedo, "Voltage sag studies in distribution networks—Part II: Voltage Sag Assessment," *IEEE Trans. Power Deliv.*, vol. 21, no. 3, pp. 1679–1688, 2006.
- [4] Z. Wang, X. Wang, and C. Y. Chung, "An analytical method for calculating critical voltage sag clearance time of induction motors," *IEEE Trans. Power Deliv.*, vol. 27, no. 4, pp. 2412–2414, 2012.
- [5] T. Tayjasanant, C. Li, and W. Xu, "A Resistance sign-based method for voltage sag," vol. 20, no. 4, pp. 2544–2551, 2005.
- [6] J. Pedra, S. Bogarra, F. Córcoles, L. Monjo, and A. Rolán, "Testing of three-phase equipment under voltage sags," *IET Electr. Power Appl.*, vol. 9, no. 4, pp. 287–296, 2015.
- [7] L. Guasch, F. Córcoles, and J. Pedra, "Effects of symmetrical and unsymmetrical voltage sags on induction machines," *IEEE Trans. Power Deliv.*, vol. 19, no. 2, pp. 774–782, 2004.
- [8] M. H. J. Bollen, "Characterisation of voltage sags experienced by three-phase adjustable-speed drives," *IEEE Trans. Power Deliv.*, 1997.
- [9] M. H. J. Bollen, "Assessment of the number of voltage sags experienced by a large industrial customer," *IEEE Trans. Ind. Appl.*, 1997.
- [10] J.A. Martinez-Velasco and J. Martin-Arnedo, "EMTP model for analysis of distributed generation impact on voltage sags," *IET Gener. Transm. Distrib.*, vol. 1, no. 1, pp. 112–119, 2007.
- [11] S. Rönnberg and M. Bollen, "Power quality issues in the electric power system of the future," *Electr. J.*, 2016.
- [12] CIGRE/CIREN/UIE Joint Working Group C4.110, "Voltage Dip Immunity of Equipment and Installations," *CIGRE Publ.*, no. April, pp. 1–18, 2010.
- [13] M. H. J. Bollen, "Influence of motor reacceleration on voltage sags," *IEEE Trans. Ind. Appl.*, vol. 31, no. 4, pp. 667–674, 1995.
- [14] M. Falahi, K. L. Butler-Purry, and M. Ehsani, "Induction motor starting in islanded microgrids," *IEEE Trans. Smart Grid*, 2013.
- [15] L. Zhang and M. H. J. Bollen, "Characteristic of voltage dips (sags) in power systems," *IEEE Trans. Power Deliv.*, vol. 15, no. 2, pp. 827–832, 2000.
- [16] Y. Wang, A. Bagheri, M. H. J. Bollen, and X. Y. Xiao, "Single-Event Characteristics for voltage dips in three-phase systems," *IEEE Trans. Power Deliv.*, vol. 32, no. 2, pp. 832–840, 2017.
- [17] M. H. J. Bollen, S. Bahramirad, and A. Khodaei, "Is there a place for power quality in the smart grid?," in *Proceedings of International Conference on Harmonics and Quality of Power, ICHQP*, 2014.
- [18] M. H. J. Bollen, J. Zhong, F. Zavoda, J. Meyer, A. McEachern, and F. Córcoles López, "Power quality aspects of smart grids," *Int. Conf. Renew. Energies Power Qual. (ICREPO'10)*, Granada 23-25 March, 2010, 2010.
- [19] Di. Chakravorty, B. Chaudhuri, and S. Y. R. Hui, "Rapid Frequency Response from Smart Loads in Great Britain Power System," *IEEE Trans. Smart Grid*, vol. 8, no. 5, pp. 2160–2169, 2017.
- [20] IEEE Standards Coordinating Committee 21, *IEEE Application Guide for IEEE Std 1547™, IEEE Standard for Interconnecting Distributed Resources with Electric Power Systems*, no. April. 2009.
- [21] A. R. Blanco, "Estudio del efecto de los huecos de tension en el generador de induccion doblemente alimentado," PhD Thesis dissertation, UPC, Terrassa 2013.
- [22] M. H. J. Bollen, "Voltage recovery after unbalanced and balanced voltage dips in three-phase systems," *IEEE Trans. Power Deliv.*, vol. 18, no. 4, pp. 1376–1381, 2003.
- [23] J. A. Martinez-Velasco and J. Martin-Arnedo, "Calculation of Voltage Sag Indices for Distribution Networks," pp. 1–6, 2005.
- [24] Ormazabal Protection and Automation, "EkorRPS-Multifunctional Protection."
- [25] The Mathworks Inc., "MATLAB 2015 - MathWorks," www.mathworks.com/products/matlab, 2016.